DOI: 10.1002/ejic.200901146

Bioconjugates of 1′-Aminoferrocene-1-carboxylic Acid with (*S*)-3-Amino-2-methylpropanoic Acid and L-Alanine

Mojca Čakić Semenčić,[a] Katja Heinze,*[b] Christoph Förster,[b] and Vladimir Rapić*[a]

Keywords: β-Amino acids / Conformation analysis / Density functional calculations / Hydrogen bonds / Metallocenes

Formal CH_2 insertion in bioconjugates composed of 1′-aminoferrocene-1-carboxylic acid (Fca) and alanine Boc-Ala-Fca-Ala-OCH_3 gives Fca bioconjugates with the β-amino acid (*S*)-3-amino-2-methylpropanoic acid (Aib). The novel homologous conjugates of ferrocene were fully characterized by spectroscopic and analytical methods. NMR, CD and IR spectroscopy in concert with DFT calculations suggest that the formal "L-Ala–to–(*S*)-β-Aib mutations" can exert ferrocene helix inversion due to the different stereogenic carbon atoms of L-Ala and (*S*)-β-Aib. Furthermore, the mutation (de-)stabilizes the conserved secondary structure with two intramolecular hydrogen bonds, depending on the "mutation site". The systematic work presented provides a firm basis for understanding the factors that determine folding in bioconjugates of ferrocene and β-amino acids and will guide the rational design of metallocene peptidomimetics incorporating β-amino acids.

Introduction

Polyamides derived from β-amino acids are one of the most extensively studied classes of peptidomimetics. β-Amino acids can be divided into three main types depending upon the position of the side chain on the 3-amino-alkanoic acid skeleton. Those with the organic residue (R) next to the amine are called β^3-amino acids, those with R next to the carbonyl group are called β^2-amino acids and those with substituents at both carbon atoms are called $\beta^{2,3}$-amino acids.

The characteristic properties of β-peptides are: (i) they fold in a predictable way to form secondary and tertiary structures, (ii) they exhibit enhanced stability towards proteolytic degradation in comparison with α-peptides, and most important (iii) they are bioactive and thus potentially useful in β-peptide-based antibiotics.[1] Depending on the amino acids employed, β-peptides adopt various structural motifs: helices, extended structures, stacks and sheets.[2] The best documented secondary structure of β-peptides is the 3_{14}-helix.[3,4] A peptide sequence consisting of 20 L-β^3-amino acids forms a (*M*)-helix stabilized by 14-membered hydrogen-bonded rings between NH and CO in a three-residue repeating arrangement.[5] The same type of helix is observed when (*S*)-β^2-amino acids are used. Peptides containing alternating β^2- and β^3-building blocks fold into a right-handed $2.7_{12,10}$-helix consisting of alternating 12- and 10-membered hydrogen-bonded rings.[6]

3-Amino-2-methylpropanoic acid (β-aminoisobutyric acid = β-Aib) is the only example of a β^2-amino acid that is present in mammalian metabolism. This nonproteinogenic amino acid is found in both enantiomeric forms. (*R*)-β-Aib is the product of the catabolism of the pyrimidine bases uracil and thymine by the enzyme dihydropyrimidine dehydrogenase constituting the first step of the pyrimidine degradation pathway. (*S*)-β-Aib plays an important role in the metabolism of α-amino acids.[7]

Understanding and control of secondary structures of proteins, peptides and oligoamides is of vital importance for designing functional peptidic materials.[8–11] The use of molecular scaffolds (templates) is a widely exploited successful method.[12] These scaffolds nucleate or propagate a certain conformation from their ordered region through subunits consisting of natural amino acids to form α-helices or β-sheet structures.

1,1′-Disubstituted ferrocene conjugates with α-amino acids or short peptides have been successfully used as redox-active scaffolds with a suitable distance between the cyclopentadienyl rings (ca. 3.3 Å) to form turn elements on the basis of intramolecular hydrogen bonding (IHB) interactions.[12,13] Turns are ubiquitous elements in the secondary structure of proteins that have become important targets in medicinal chemistry.[14–17] Symmetrically substituted bioconjugates of ferrocene-1,1′-dicarboxylic acid (Fcd) with one or two α-amino acids in both strands have been thoroughly studied. In the solid state, the majority of these compounds form two IHBs (independent of the number and

[a] Department of Chemistry and Biochemistry, Faculty of Food Technology and Biotechnology,
Pierottijeva 6, 10000 Zagreb, Croatia
Fax: +385-4836-082
E-mail: vrapic@pbf.hr
[b] Institute of Inorganic Chemistry and Analytical Chemistry, Johannes Gutenberg University of Mainz,
Duesbergweg 10–14, 55128 Mainz, Germany
Fax: +49-6131-3927277
E-mail: katja.heinze@uni-mainz.de
Supporting information for this article is available on the WWW under http://dx.doi.org/10.1002/ejic.200901146.

type of the amino acid incorporated). This double IHB results in the formation of two 10-membered rings (Scheme 1, type-I, β-turn-like "Herrick conformation"). Usually, these IHBs are sufficiently strong to retain this approximate C_2 symmetrical conformation in chloroform solution.[18–28] Unsymmetrical 1,*n*′-disubstituted ferrocenoyl amides CH_3O-Phe-Fcd-AA-OCH_3 with AA equalling achiral amino acids Gly, β-Ala or γ-Aba (Phe = phenyl alanine, Gly = glycine, β-Ala = β-alanine, γ-Aba = γ-aminobutyric acid) were shown to exhibit less stable double IHBs the more methylene groups are inserted.[28]

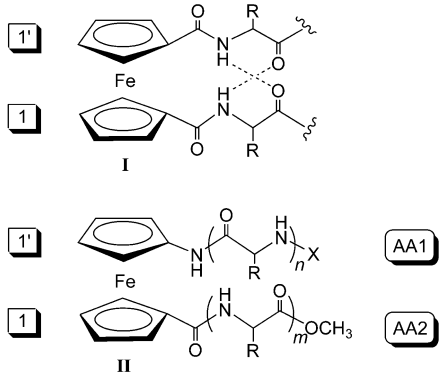

Scheme 1. Organometallic peptidomimetics derived from ferrocene-1,1′-dicarboxylic acid (Fcd, type I) and from 1′-aminoferrocene-1-carboxylic acid (Fca, type II) constructed from L- and D-amino acids, (*m*, *n* = 0, 1, 2, ...; X = Ac, Boc).

In our recent studies we focused on the preparation and conformational analysis of a number of 1′-aminoferrocene-1-carboxylic acid (Fca) bioconjugates with α-amino acids (Scheme 1, type-II bioconjugates).[29–35] Unlike Fcd derived metallocene turn structures (possessing parallel juxtaposed peptide strands) compounds of type II represent truly organometallic turn mimetics maintaining an antiparallel orientation of these subunits – as found in natural folded peptides. A prominent feature of both type I and type II peptidomimetics is the helical chirality around the ferrocene moiety, which has been amply demonstrated by X-ray crystallographic analyses. CD spectroscopy is the method of choice to determine the helical chirality of the ferrocene unit in such systems in solution. Complementary CD measurements in the solid state corroborate the findings of X-ray structural analyses. Fcd bioconjugates of type I containing L-amino acids are characterized in the solid state by two IHBs resulting in (*P*)-helicity of the ferrocene subunit. Such conformations persist in solutions of noncoordinating solvents as positive Cotton effects around the UV/Vis absorption maximum of the ferrocene chromophore ($\lambda_{max} \approx$ 455 nm) are observed. Vice versa, bioorganometallics derived from D-amino acids are characterized by negative CD signals and (*M*)-helicity.[32,33] In Fca bioconjugates composed of L-Ala and D-Ala the metallocene core chirality is determined by the configuration of the first amino acid attached to the Fca amino group.[31]

Fca bioconjugates of type II can be divided into two subgroups with distinct conformational preferences. Bis(amide)s composed of Fca and a single α-amino acid attached at the *C*-terminal side of Fca form a library of several conformational isomers in solution.[29–31,34,35] The main features of these bis(amide)s are: (i) increasing the steric bulk of the amino acid incorporated disfavours some energetically accessible conformers; (ii) changing the solvent from CH_2Cl_2 to CH_3CN promotes some conformers over others and (iii) self-association dominates the conformational preferences in the solid state. Tris(amide)s with Fca located *in between two* α-amino acids (as well as within tetra- and pentaamides[30,31]) feature different conformational and chiroptical properties. These larger peptides are well described by a single conformer which is highly stabilized by two IHBs irrespective of the size of protecting group (Ac, Boc), the size of the side chain of the amino acids and the medium (solid state/solution). One IHB spans NH(Fc) to CO(AA2) forming a nine-membered ring and the other one connects NH(AA2) to CO(Ac) or CO(Boc), respectively, giving an 11-membered ring.

Given the characteristics and diversities in hydrogen-bonding motifs found in type-II bioconjugates of Fca and α-amino acids as well as the interesting secondary and tertiary structures of folded β-peptides novel bioconjugates of Fca and (*S*)-3-amino-2-methylpropanoic acid [(*S*)-β-Aib] and mixed conjugates of Fca and β-Aib/Ala are targeted and studied in this report. In other words, we are interested in the effect of formal CH_2 group insertion in the backbone of the amino acid substituents AA1/AA2 on the hydrogen-bonding pattern of Fca amino acid bioconjugates (Ala/β-Aib permutation).

Results and Discussion

Synthesis and Characterization of Bioconjugates of Fca and Aib

The required starting materials 1′-(*tert*-butoxycarbonylamino)ferrocene-1-carboxylic acid (Boc-Fca, **1**),[36] Boc-Fca-Ala-OCH_3 (**5**)[33] and (*S*)-3-amino-2-methylpropanoic acid (β-Aib, 93% *ee*)[37] were prepared according to literature procedures. The synthetic procedure for the assembly of mixed AA1-Fca-AA2 conjugates with AA1, AA2 = β-Aib or α-Ala conjugates is outlined in Scheme 2. β-Aib-OCH_3 is coupled to Boc-protected ferrocene amino acid **1** using the EDC/HOBt protocol to give the Boc-Fca-Aib-OCH_3 conjugate **2** in 78% isolated yield [EDC = *N*-(3-dimethylaminopropyl)-*N*′-ethylcarbodiimide hydrochloride; HOBt = 1-hydroxybenzotriazole]. After removal of the Boc protecting group of **2** by hydrochloric acid, Boc-β-Aib is coupled – again using the EDC/HOBt method – to give Boc-Aib-Fca-Aib-OCH_3 conjugate **3** in 53% isolated yield. Similarly, Boc-Ala is attached to **2** to give Boc-Ala-Fca-Aib-OCH_3 conjugate **4** in 65% yield. Finally, the Boc-Aib-Fca-Ala-OCH_3 derivative **6** is obtained from Boc-Fca-Ala-OCH_3 **5** by attachment of Boc-Aib in 73% yield.

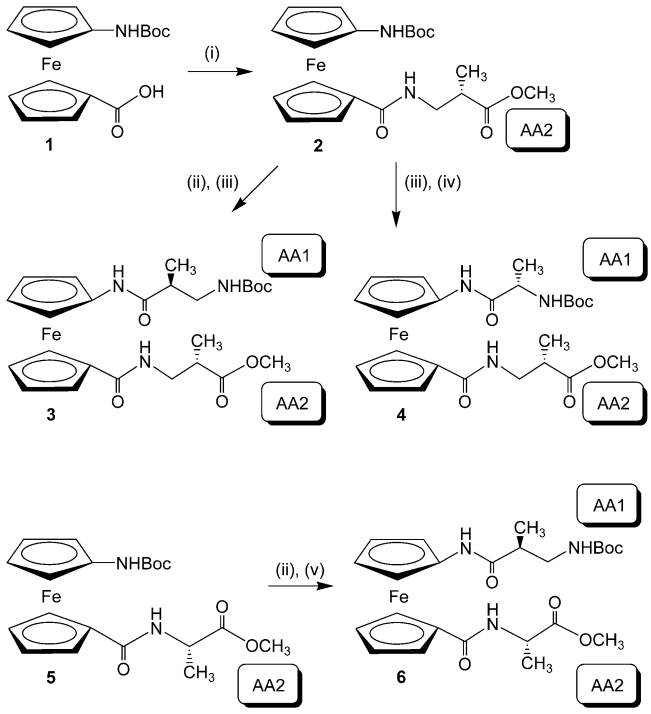

Scheme 2. Synthesis of β-Aib conjugates of Fca. (i) 1. HOBt, EDC, CH_2Cl_2; 2. β-Aib-OCH_3·HCl, CH_2Cl_2, NEt_3; (ii) HCl(g)/ethyl acetate; (iii) 1. Boc-β-Aib-OH, HOBt, EDC, CH_2Cl_2; 2. **2**·HCl, CH_2Cl_2, NEt_3; (iv) 1. Boc-Ala-OH, HOBt, EDC, CH_2Cl_2; 2. **2**·HCl, CH_2Cl_2, NEt_3; (v) 1. Boc-β-Aib-OH, HOBt, EDC, CH_2Cl_2; 2. **5**·HCl, CH_2Cl_2, NEt_3.

The proposed composition and purity of the organometallic amides **2**, **3**, **4** and **6** is verified by mass spectrometry and elemental analysis (see Exp. Sect.). Proton NMR spectra of **3**, **4** and **6** show only a single set of resonances suggesting only the presence of one diastereomer and thus the integrity of the two stereogenic carbon centres of the (*S*)-β-Aib and L-Ala residues, i.e. no racemization is observed under these conditions.

As usually observed for ferrocene complexes a reversible one-electron oxidation assigned to the ferrocene/ferrocenium couple can be observed for all new compounds. The redox potential of **2**, **3**, **4** and **6** is almost independent on the remote substituents (see Exp. Sect.).

In the IR spectra of **2**, **3**, **4** and **6** characteristic group frequencies are observed for NH and CO groups (Tables 1 and 2). In the solid state as KBr disk, the low-energy NH stretching vibrations below $\tilde{\nu} = 3400\ cm^{-1}$ indicate that all NH groups are hydrogen-bonded. The bands for the ester carbonyl stretching vibrations CO(AA2) in the solid state suggest hydrogen bonds to the ester carbonyl groups CO(AA2) in **2** and **4** but not in **3** and **6** (Table 1). In CH_2Cl_2 solution, bioconjugates **2**–**4** feature quite strongly hydrogen-bonded ester carbonyl groups CO(AA2) while **6** features only weakly bonded CO(AA2) groups. All bioconjugates exhibit free and hydrogen-bonded NH groups in solution according to the presence of absorption bands below $3400\ cm^{-1}$ and above $3400\ cm^{-1}$ (Table 2). The ratio of the two discernible NH stretching vibrations (free/bonded) characterizing compounds **2**, **3**, **4** and **6** remains unchanged upon dilution from $c = 10^{-2}$ M to 10^{-3} M suggesting that some NH groups form *intramolecular* hydrogen bonds (IHBs) rather than *intermolecular* hydrogen bonds under these conditions.

Table 1. IR spectroscopic data (in KBr) of **2**, **3**, **4** and **6** [$\tilde{\nu}/cm^{-1}$].

	NH_{bonded}	CO(AA2)	Amide I	Amide II
2	3310	1723	1699, 1634	1547
3	3287	1736	1688, 1671, 1630	1547
4	3294	1713	1688, 1633	1562, 1546
6	3294	1744	1692, 1634	1536

Table 2. IR spectroscopic data ($c = 10^{-2}$ M in CH_2Cl_2) of **2**, **3**, **4** and **6** [$\tilde{\nu}/cm^{-1}$].

	NH_{free}	NH_{bonded}	CO(AA2)	Amide I	Amide II
2	3438	3344	1723	1652	1531
3	3446	3309	1711	1686, 1652	1523
4	3436	3399, 3329	1714	1697, 1650	1559, 1526, 1501
6	3444	3355	1733	1685, 1652	1557, 1515

However, a detailed assignment to individual NH groups is impossible by IR spectroscopic methods alone. Thus, proton NMR spectroscopy was employed to elaborate which NH groups form IHBs in the β-amino acid derivatives, namely NH(Fc), NH(AA1) and/or NH(AA2).

All proton and carbon resonances were observed in expected regions (see Exp. Sect.). It is noticed that the attachment point of Aib at Fca slightly influences its *C*H, CH_2 and CH_3 resonances. Complexes with AA1 = Aib show ^{13}C resonances at lower field than complexes with AA2 = Aib which allows full assignment on the basis of simple comparison (Table 3). For conjugates **3**, **4** and **6** eight discernible *C*H(Cp) resonances are observed suggesting chirality information transfer from the substituents to the ferrocene core while **2** features only seven distinguishable *C*H(Cp) signals (see Exp. Sect.). A similar situation is found for the *H*(Cp) resonances of **2**, **3**, **4** and **6** (see Exp. Sect.).

Table 3. Selected ^1H NMR and ^{13}C NMR spectroscopic data of **2**, **3**, **4** and **6** in $CDCl_3$ ($c = 10^{-1}$ M) [δ/ppm].

	2	**3**	**4**	**6**
N*H*(Fc)	6.32	7.73	8.44	8.04
N*H*(AA1)	–	5.54	5.32	5.51
N*H*(AA2)	6.66	6.76	7.07	6.79
*C*H(Aib)	39.63	39.61, 41.52	40.68	41.41
CH_2(Aib)	42.01	42.05, 43.74	42.52	43.33
CH_3(Aib)	15.00	15.01, 15.54	15.00	15.20

The chemical shifts of the NH protons allow a tentative suggestion as to whether the respective proton is involved in a hydrogen bond.[31–35] From Table 3 it is seen that NH(Fc) forms hydrogen bonds with increasing relevance in the series **2** < **3** < **6** < **4**. Similarly, NH(AA2) of **4** forms hydrogen bonds while NH(AA1) appears practically non-bonding in all cases. Thus the NMR spectroscopic data suggest quite strong hydrogen bonds involving NH(Fc) and NH(AA2) for **4** and less important hydrogen bonds for **3** and **6** and practically no (or very weak) hydrogen bonds for **2**.

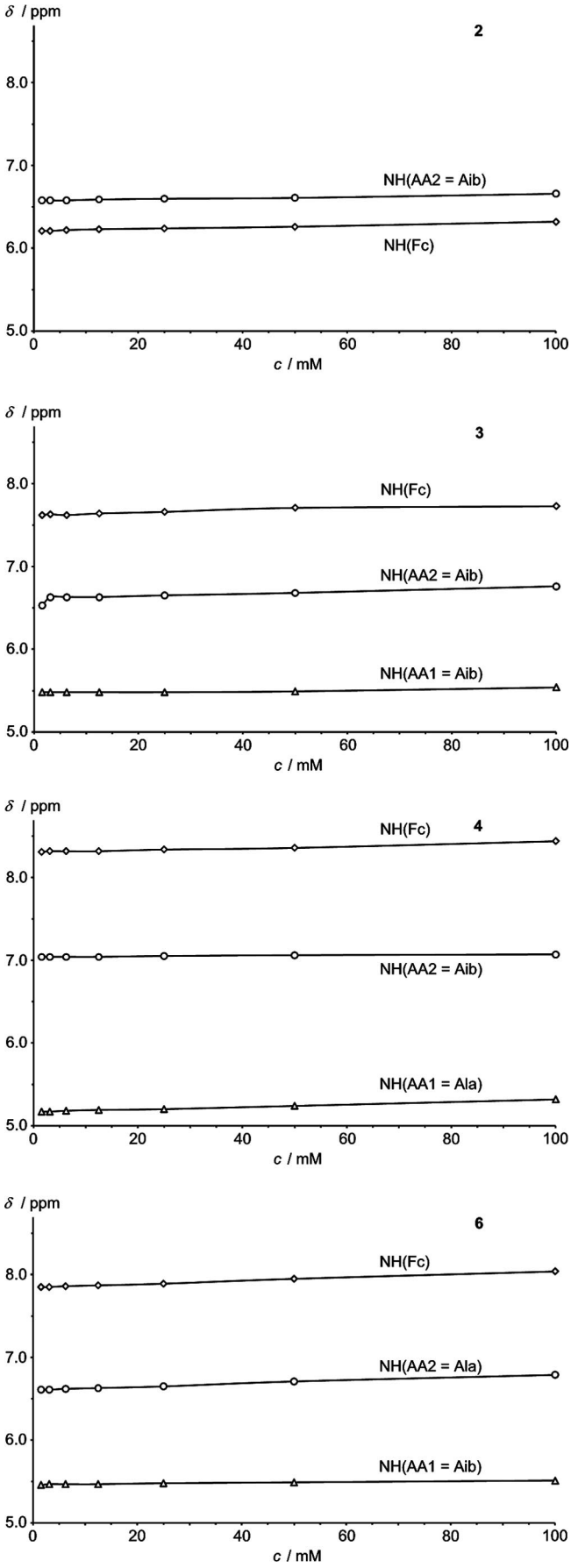

Figure 1. δ vs. c plot of NH resonances of **2**, **3**, **4** and **6** in $CDCl_3$.

NMR spectroscopic dilution experiments in the concentration range 1.5–100 mM reveal that in all cases hydrogen bonding is *intramolecular* in nature as the chemical shifts of the NH protons are independent of the concentration (Figure 1).

CD spectra of **2**, **3**, **4** and **6** were recorded in CH_2Cl_2 solution in order to access the degree of chirality induction, namely the helicity of the ferrocene moiety (Table 4, Figure 2). The (absolute) Cotton effects at the ferrocene absorption around 445 nm[12] increase in the series **2** < **3** < **6** < **4**. Interestingly, the measured Cotton effects are positive for **4** (similar to that of Ala-Fca-Ala derivatives[31]) and negative for **3** and **6** both in solution and in the solid state. Additional spectra were recorded in the presence of IHB destabilizing DMSO (20% v/v) as a competitive solvent. The CD pattern is conserved in all cases, the absolute CD signal intensity, however, is reduced significantly indicating destabilization of the secondary structures in the presence of DMSO (Table 4).

Table 4. UV/Vis and CD spectroscopic data of **2**, **3**, **4** and **6** in CH_2Cl_2 and in CH_2Cl_2/DMSO (20% v/v) ($c = 5.5 \times 10^{-4}$ M).[a]

	2	**3**	**4**	**6**
λ_{max} (ε)[b]	443 (1370)	445 (1180)	443 (1200)	443 (1165)
λ_{max} (ε)[c]	443 (1125)	443 (1190)	443 (1180)	443 (1125)
λ_{max} (M_θ)[b]	481 (8260)	460 (–14300)	466 (50510)	483 (–29710)
λ_{max} (M_θ)[c]	490 (2700)	463 (–8890)	464 (14840)	478 (–17920)
λ_{max} (CD)[d]	n.o.	470 (neg.)	470 (pos.)	480 (neg.)

[a] The units are as follows: λ_{max} [nm], (ε [$M^{-1}cm^{-1}$]); M_θ [° $M^{-1}cm^{-1}$]. [b] In CH_2Cl_2. [c] In CH_2Cl_2/DMSO (20% v/v). [d] As KBr disk.

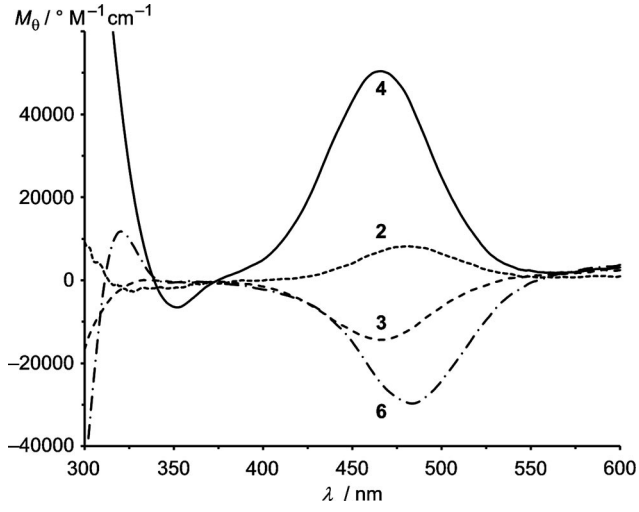

Figure 2. CD spectra of **2**, **3**, **4** and **6** in CH_2Cl_2 solution ($c = 5.5 \times 10^{-4}$ M).

The combined experimental data of **2** – namely weak differentiation of proton and carbon Cp resonances, absence of strong hydrogen bonds to CO(AA2) (very weak IHBs at best) and a weak CD signal – suggest that **2** bearing only the chiral β-amino acid Aib at the C-terminus of Fca (AA2 position) is not strongly organized in solution.

For **3**, **4** and **6** the data suggest some degree of chiral ordered conformations with NH(Fc) preferentially hydrogen bonded to CO(AA2), significant discrimination of proton and carbon Cp resonances and quite strong Cotton effects. NH(AA1) of all β-amino acid conjugates appears practically not hydrogen-bonded in solution. Proton NMR and CD spectroscopic evidence suggests that the stability of the preferred conformations increases from **3** < **6** < **4**.

The sign of the Cotton effects observed obviously depends on the stereochemistry of AA1. With AA1 = L-Ala a positive Cotton effect and hence a positive ferrocene helicity is induced while with AA1 = (*S*)-β-Aib a negative Cotton effect and hence a (*M*) ferrocene helix is found. Thus, the configuration of the stereogenic carbon atom of the amino acid at the *N*-terminal side determines the helicity of the ferrocene – an observation previously made also for Ala-Fca-Ala derivatives based on L-Ala and D-Ala.[31]

DFT Modelling of Bioconjugates of Fca and Aib

In order to put these pieces of information into a consistent picture conformational analyses with theoretical methods were attempted. Several conformations with varying IHBs of **2**, **3**, **4** and **6** were optimized at the B3LYP, LanL2DZ level of theory and their relative energies were determined (see Supporting Information).

Conjugate **2** with one single Aib unit and a Boc-protected amine substituent can only form a single IHB between these substituents. In some conformations an additional contact NH(AA2)···OC(AA2) within the Aib moiety is possible. However, no significant conformational preferences are introduced by the remote chiral carbon atom of Aib as all calculated conformers possess similar energies within 10 kJ mol^{-1} and the pseudo enantiomers with (*P*)/(*M*) helical ferrocenes are similar within 3 kJ mol^{-1} (see Supporting Information). This agrees with the weak Cotton effect observed for **2** (Table 4).

The bis(Aib) conjugate **3** features considerably more possibilities for IHBs between and within the ferrocene substituents. A conformation similar to the highly stabilized system of Ala-Fca-Ala derivatives with two IHBs is also a stable minimum for **3** (Figure 3, Scheme 3; for other local geometrical minima of **3** see Supporting Information). One IHB spans NH(Fc) to CO(AA2) forming a 10-membered ring and the other one connects NH(AA2) to CO(Boc) giving a 12-membered ring. Thus both rings are expanded by one atom relative to those of triamides composed of Fca and Ala (9/11 ring pattern). The involvement of CO(AA2) is also consistent with the IR data of **3** (Table 2). The conformation with two IHBs showing a negative ferrocene helicity (with torsion angle C_{ipso}–$C_{centroid}$–$C_{centroid}$–C_{ipso} –61°) is slightly more stabilized than the one with positive ferrocene helicity of 67° by 8.2 kJ mol^{-1} (Figure 3) which accounts for the observed negative Cotton effect of **3** (Table 4). The enhanced stability is also reflected in the shorter N*H*···*O*C IHB distances in the (*M*)-helical conformer as compared to those of the (*P*)-helical conformer (Figure 3).

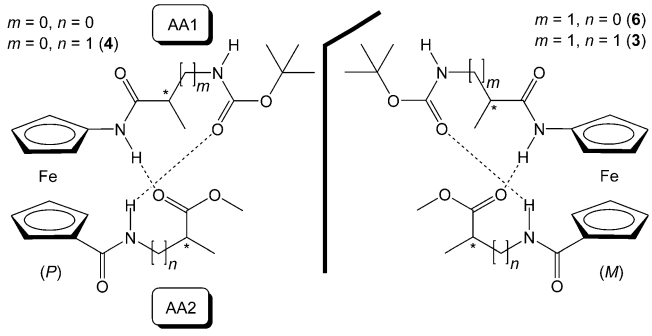

Scheme 3. Most prevalent conformations of Aib–ferrocene bioconjugates in solution.

The double IHB motif spanning the substituents is also found as the minimum geometry of Ala-Fca-Aib derivative **4** (Figure 4, Scheme 3; for other local geometrical minima of **4** see Supporting Information). The IHBs form a 10/11 ring pattern. Interestingly, the pseudo enantiomer with a (*P*)-helical ferrocene is significantly stabilized relative to the (*M*)-helical conformation by 17.7 kJ mol^{-1} accounting for the observed large *positive* Cotton effect of **4** (Table 4, Fig-

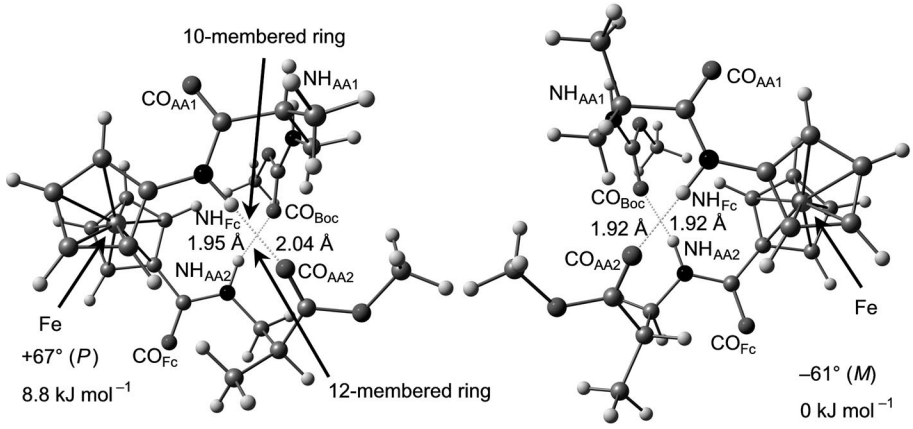

Figure 3. DFT-calculated conformations of **3** with two IHBs and with positive and negative ferrocene helicity and some relevant metrical parameters.

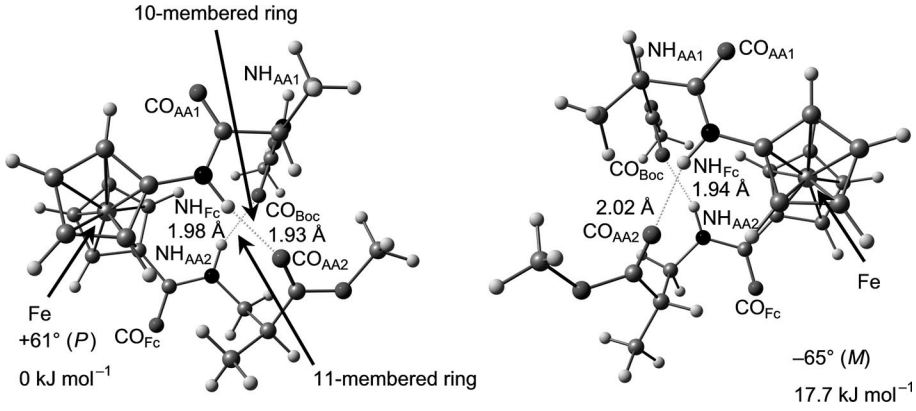

Figure 4. DFT-calculated conformations of **4** with two IHBs and with positive and negative ferrocene helicity and some relevant metrical parameters.

ure 2). The shorter N*H*···*O*C IHB distances in the (*P*)-helical conformer are compatible with its greater stability. Again, the experimental carbonyl stretching vibration CO(AA2) of **4** is in line with the calculated IHB to CO(AA2) (Table 2, Figure 4).

For Aib-Fca-Ala conjugate **6** the double IHB motif is also calculated as minimum geometry with 9- and 12-membered rings (Figure 5, top, Scheme 3). The calculated energy difference between the pseudo enantiomers amounts to only 6.2 kJ mol^{-1} with the (*P*)-helix being slightly stabilized (inconsistent with the experimental negative Cotton effect, Table 4). However, an additional quite stable conformation with two IHBs resulting in 9- and 10-membered rings is also detected during the optimizations (Figure 5, bottom). In this conformation the (*M*)-helix is significantly stabilized relative to the (*P*)-helical ferrocene which could account for the observed negative CD signal of **6** (Figure 2).

These theoretically derived results are congruent with the experimental observations: **4** features the most stabilized ordered conformation in the Fca-Aib conjugates described. In all cases the double IHB motif appears to be a relevant conformation in solution (Scheme 3), which is especially pronounced for **4** (m = 0, n = 1) and several known Ala-Fca-Ala derivatives with $m = n = 0$.[31] Elongating AA2 from Ala to (*S*)-β-Aib ($n = 0 \rightarrow 1$) (with concomitant inversion of the stereogenic carbon atom) disturbs neither the conformational stability nor the helicity of the ferrocene (**4**). However, elongating AA1 from Ala to (*S*)-β-Aib (m =

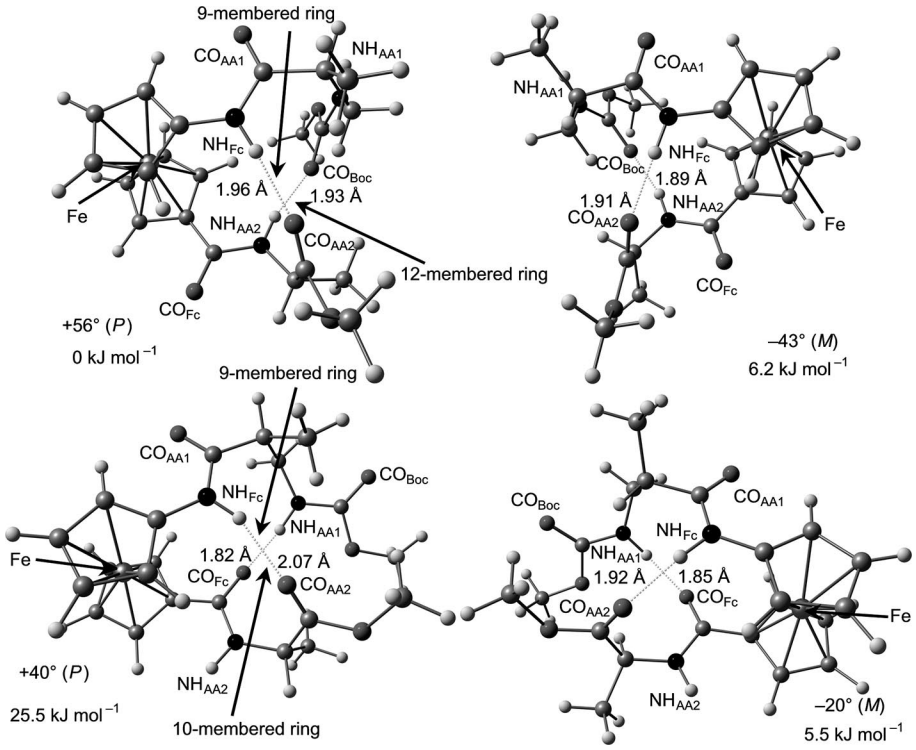

Figure 5. DFT-calculated conformations of **6** with two IHBs and with positive and negative ferrocene helicity and some relevant metrical parameters.

$0 \rightarrow 1$) has quite a destabilizing effect on the folded conformation and results in helix inversion at the ferrocene (**3** and **6**). For **6** an additional conformation with two different IHBs appears to play a significant role (9/10 ring pattern).

Conclusions

Starting conceptually from Boc-Ala-Fca-Ala-OCH_3 ($m = n = 0$), formal methylene insertion at the *C*-terminal side [AA2 = (*S*)-β-Aib; $n = 1$] to afford Boc-Ala-Fca-Aib-OCH_3 (**4**) conserves the stable ordered conformation with two IHBs and a positive helical ferrocene unit (*P*).

Formal methylene insertion at the *N*-terminal side [AA1 = (*S*)-β-Aib; $m = 1$] starting from Boc-Ala-Fca-Ala-OCH_3 to afford Boc-Aib-Fca-Ala-OCH_3 (**6**) opens up new opportunities and conformational flexibility resulting in a destabilized ordered conformation and a preferred helix inversion at the ferrocene (*M*) due to the different stereochemistry at the chiral carbon atom of (*S*)-β-Aib relative to that of Ala.

Double methylene insertion giving Boc-Aib-Fca-Aib-OCH_3 (**3**) strongly destabilizes the double IHB motif relative to other conformations and results in helix inversion of the ferrocene (*M*). Thus, the helicity of the ferrocene appears to be governed by the configuration of the carbon atom of AA1 in AA1-Fca-AA2 conjugates both for α-amino acids and for β-amino acids.

Experimental Section

General: Most synthetic procedures were carried out under argon. CH_2Cl_2 used for synthesis and spectroscopy was dried (P_2O_5), distilled from CaH_2 and stored over molecular sieves (4 Å). EDC [EDC = *N*-(3-dimethylaminopropyl)-*N*′-ethylcarbodiimide hydrochloride, Aldrich] and HOBt (HOBt = 1-hydroxybenzotriazole, Aldrich) were used as received. 1′-(*tert*-butoxycarbonylamino)ferrocene-1-carboxylic acid (Boc-Fca, **1**),[36] Boc-Fca-Ala-OCH_3 (**5**)[33] and (*S*)-3-amino-2-methyl propanoic acid (β-Aib)[37] were prepared using previously described procedures. The enantiomeric excess *ee* of (*S*)-β-Aib (*ee* = 93%) was determined after conversion in **2** by using a Chiralcel OD-H column (Knauer model K-2501 pump and K-501 detector) in *n*-hexane/isopropanol mixture at a 1 mL min^{-1} flow rate. Products were purified by preparative thin layer chromatography on silica gel (Merck, Kieselgel 60 HF254) using CH_2Cl_2/ethyl acetate mixtures. Melting points were determined with a Reichert Thermovar HT 1 BT 11 melting point apparatus. IR spectra were recorded as CH_2Cl_2 solutions and KBr pellets with a Bomem MB 100 mid FTIR spectrophotometer. FD mass spectra were recorded with a FD Finnigan MAT90 spectrometer. HR-ESI mass spectra were recorded with a Micromass Q-TOF-Ultima-API spectrometer. UV/Vis and CD spectra were recorded using a Jasco-810 spectropolarimeter in CH_2Cl_2 or CH_2Cl_2/DMSO mixtures and KBr pellets. ^{1}H and ^{13}C NMR spectra were recorded with a Bruker Avance 600 MHz spectrometer in $CDCl_3$ solution with Me_4Si as internal standard. Electrochemical experiments were carried out with a BioLogic SP-50 voltammetric analyzer using a glassy carbon working electrode, a platinum wire as counter electrode and a 0.01 M $Ag/AgNO_3$ electrode as reference electrode [(nBu$_4$N)(ClO_4) in CH_3CN]. The measurements were carried out at a scan rate of 100 mV s^{-1} for cyclic voltammetry experiments and at 250 mV s^{-1} for square-wave voltammetry experiments using 0.1 M (nBu$_4$N)(PF_6) as supporting electrolyte in CH_2Cl_2. Potentials are given relative to the ferrocene/ferrocenium couple ($E_{1/2}$ = 220 ± 5 mV under the experimental conditions).

Computational Methods: Density functional calculations were carried out with the Gaussian03/DFT[38] series of programs. The B3LYP formulation of density functional theory was used employing the LanL2DZ basis set.[38] All points were characterized as minima ($N_{imag} = 0$) by frequency analysis.

Boc-Fca-(*S*)-β-Aib-OCH_3 (2): Boc-Fca (**1**, 310 mg, 0.9 mmol) was activated using EDC (207 mg, 1.08 mmol) and HOBt (150 mg, 1.08 mmol) and (*S*)-β-Aib-OCH_3 [obtained from (*S*)-β-Aib-OCH_3·HCl, 274.5 mg, 1.8 mmol by treatment with Et_3N in CH_2Cl_2, pH ≈ 8] was added. The mixture was stirred for two hours at room temperature, washed with a saturated aqueous solution of $NaHCO_3$, a 10% aqueous solution of citric acid and H_2O, dried with Na_2SO_4 and the solvents were evaporated in vacuo. TLC purification of the crude product with CH_2Cl_2/ethyl acetate (10:1) gave conjugate **2** (320 mg, 78%) as orange crystals. M.p. 41 °C. $C_{21}H_{28}FeN_2O_5$ (444.31): calcd. C 56.77, H 6.35, N 6.30; found C 57.03, H 6.13, N 6.45. MS (FD): *m*/*z* (%) = 443.7 (100) $[M]^+$, 887.6 (32) $[M_2]^+$. MS (HR-ESI$^+$): calcd. for $C_{21}H_{28}N_2O_5{}^{23}Na^{54}Fe$ 465.1292; found 465.1296. ^{1}H NMR ($CDCl_3$, 600 MHz): δ = 6.66 [br.s, 1 H, NH(AA2)], 6.32 [s, 1 H, NH(Fca)], 4.60 (s, 1 H, Cp-H), 4.56 (s, 1 H, Cp-H), 4.39 (s, 1 H, Cp-H), 4.36 (s, 1 H, Cp-H), 4.32 (pt, 2 H, Cp-H), 3.98 (pt, 2 H, Cp-H), 3.72 (s, 3 H, OCH_3), 3.62 [m, 1 H, CH_2(Aib)], 3.42 [m, 1 H, CH_2(Aib)], 2.86 [m, 1 H, CH(Aib)], 1.49 [s, 9 H, CH_3(Boc)], 1.23 [d, $^3J_{HH}$ = 7.20 Hz, 3 H, CH_3(Aib)] ppm. ^{13}C{^{1}H} NMR ($CDCl_3$, 150 MHz): δ = 175.68 [s, CO(ester)], 169.76 [s, CO(Fca)], 153.23 [s, CO(Boc)], 96.28 (s, Cp-C_q), 80.17 [s, C(Boc)], 77.62 (s, Cp-C_q), 71.07 (s, Cp-C), 71.03 (s, Cp-C), 69.29 (s, Cp-C), 69.25 (s, Cp-C), 65.82 (2s, 2 Cp-C), 63.06 (s, Cp-C), 62.95 (s, Cp-C), 51.93 (s, OCH_3), 42.01 [s, CH_2(Aib)], 39.63 [s, CH(Aib)], 28.34 [s, CH_3(Boc)], 15.00 [s, CH_3(Aib)] ppm. CV (CH_2Cl_2): $E_{1/2}$ = 40 mV vs. Fc/Fc^+.

Boc-(*S*)-β-Aib-Fca-(*S*)-β-Aib-OCH_3 (3): A suspension of **2** (170 mg, 0.383 mmol) in ethyl acetate (7 mL) was cooled to 0 °C and treated with gaseous HCl for two hours. The mixture was evaporated to dryness and the resulting hydrochloride was treated with Et_3N in CH_2Cl_2 (pH ≈ 8). The free amine was coupled with Boc-(*S*)-β-Aib-OH (155.5 mg, 0.766 mmol) (activated by using the standard EDC/HOBt method). The mixture was stirred for three hours at room temperature, washed with a saturated aqueous solution of $NaHCO_3$, a 10% aqueous solution of citric acid and H_2O, dried with Na_2SO_4 and the solvents evaporated in vacuo. TLC-purification of the crude product with CH_2Cl_2/ethyl acetate (10:1) gave conjugate **3** (87 mg, 53%) as orange crystals. M.p. 117 °C. $C_{25}H_{35}FeN_3O_6$ (529.42): calcd. C 56.72, H 6.66, N 7.94; found C 56.60, H 6.73, N 8.03. MS (FD): *m*/*z* (%) = 528.8 (46) $[M]^+$, 551.7 (32) $[M + Na]^+$, 1057.8 (23) $[M_2]^+$, 1080.8 (100) $[M_2 + Na]^+$, 1094.8 (28) $[M_2 + K]^+$. MS (HR-ESI$^+$): calcd. for $C_{25}H_{35}N_3O_6{}^{23}Na^{54}Fe$ 550.1820; found 550.1796. ^{1}H NMR ($CDCl_3$, 600 MHz): δ = 7.73 [s, 1 H, NH(Fca)], 6.76 [br.s, 1 H, NH(Aib2)], 5.54 [br.s, 1 H, NH(Aib1)], 4.61 (s, 1 H, Cp-H), 4.56 (s, 1 H, Cp-H), 4.53 (s, 1 H, Cp-H), 4.36 (s, 3 H, Cp-H), 4.07 (s, 2 H, Cp-H), 3.76 (s, 3 H, OCH_3), 3.73–3.29 [m, 4 H, CH_2(Aib1 + Aib2)], 2.91 [m, 1 H, CH(Aib2)], 2.70 [m, 1 H, CH(Aib1)], 1.45 [s, 9 H, CH_3(Boc)], 1.27 [d, $^3J_{HH}$ = 7.14 Hz, 3 H, CH_3(Aib2)], 1.24 [d, $^3J_{HH}$ = 6.99 Hz, 3 H, CH_3(Aib1)] ppm. ^{13}C{^{1}H} NMR ($CDCl_3$, 150 MHz): δ = 176.44 [s, CO(ester)], 174.20 [s, CO(amide)], 170.42 [s, CO(Fca)], 156.33 [s, CO(Boc)], 94.26 (s, Cp-C_q), 79.33 [s, C(Boc)], 77.59 (s, Cp-C_q), 71.12 (s, Cp-C), 71.02 (s, Cp-C), 69.97 (s, Cp-C), 69.42 (s, Cp-C),

66.31 (s, Cp-C), 66.01 (s, Cp-C), 64.51 (s, Cp-C), 64.13 (s, Cp-C), 52.04 (s, OCH_3), 43.74 [s, CH_2(Aib1)], 42.05 [s, CH_2(Aib2)], 41.52 [s, CH(Aib1)], 39.61 [s, CH(Aib2)], 28.44 [s, CH_3(Boc)], 15.54 [s, CH_3(Aib1)], 15.01 [s, CH_3(Aib2)] ppm. CV (CH_2Cl_2): $E_{1/2}$ = 90 mV vs. Fc/Fc^+.

Boc-Ala-Fca-(*S*)-β-Aib-OCH$_3$ (4): In a same manner as described for **3**, activated Boc-Ala-OH (189 mg, 0.676 mmol) was coupled with deprotected **2** (170 mg, 0.338 mmol) giving 113 mg (65%) of **4** as orange crystals. M.p. 60 °C. $C_{24}H_{33}FeN_3O_6$ (515.39): calcd. C 55.93, H 6.45, N 8.15; found C 56.04, H 6.33, N 8.28. MS (FD): *m/z* (%) = 514.7 (100) $[M]^+$, 1052.6 (24) $[M_2 + Na]^+$. MS (HR-ESI$^+$): calcd. for $C_{24}H_{33}N_3O_6{}^{23}Na^{54}Fe$ 536.1663; found 536.1674. ^{1}H NMR ($CDCl_3$, 600 MHz): δ = 8.44 [s, 1 H, NH(Fca)], 7.07 [br.s, 1 H, NH(Aib)], 5.32 [d, $^3J_{HH}$ = 6.36 Hz, 1 H, NH(Ala)], 4.89 (s, 1 H, Cp-H), 4.69 (s, 1 H, Cp-H), 4.43 (s, 2 H, Cp-H), 4.29 (s, 2 H, Cp-H), 4.19 [m, 1 H, CH(Ala)], 4.08 (s, 1 H, Cp-H), 4.00 (s, 1 H, Cp-H), 3.82 [m, 1 H, CH_2(Aib)], 3.78 (s, 3 H, OCH_3), 3.34 [m, 1 H, CH_2(Aib)], 2.89 [m, 1 H, CH(Aib)], 1.46 [s, 9 H, CH_3(Boc)], 1.42 [d, $^3J_{HH}$ = 6.90 Hz, 3 H, CH_3(Ala)], 1.26 [d, $^3J_{HH}$ = 7.10 Hz, 3 H, CH_3(Aib)] ppm. $^{13}C\{^1H\}$ NMR ($CDCl_3$, 150 MHz): δ = 176.73 [s, CO(ester)], 171.83 [s, CO(amide)], 170.65 [s, CO(Fca)], 156.08 [s, CO(Boc)], 95.10 (s, Cp-C_q), 80.49 [s, C(Boc)], 77.27 (s, Cp-C_q), 71.80 (s, Cp-C), 70.70 (s, Cp-C), 70.02 (s, Cp-C), 69.67 (2s, Cp-C), 65.94 (s, Cp-C), 64.25 (s, Cp-C), 63.10 (s, Cp-C), 52.24 (s, OCH_3), 51.03 [s, CH(Ala)], 42.52 [s, CH_2(Aib)], 40.68 [s, CH(Aib)], 28.53 [s, CH_3(Boc)], 18.17 [s, CH_3(Ala)], 15.00 [s, CH_3(Aib)] ppm. CV (CH_2Cl_2): $E_{1/2}$ = 110 mV vs. Fc/Fc^+.

Boc-(*S*)-β-Aib-Fca-Ala-OCH$_3$ (6): Using the procedure applied for **3**, activated Boc-(*S*)-β-Aib-OH (203 mg, 0.956 mmol) was coupled with deprotected **5** (205 mg, 0.478 mmol) giving 180 mg (73%) of **6** as orange crystals. M.p. 66 °C. $C_{24}H_{33}FeN_3O_6$ (515.39): calcd. C 55.93, H 6.45, N 8.15; found C 56.07, H 6.38, N 8.20. MS (FD): *m/z* (%) = 440.7 (100) $[M - OC_4H_{10}]^+$, 514.7 (24) $[M]^+$. MS (HR-ESI$^+$): calcd. for $C_{24}H_{33}N_3O_6{}^{23}Na^{54}Fe$ 536.1663; found 536.1656. ^{1}H NMR ($CDCl_3$ 600 MHz): δ = 8.04 [s, 1 H, NH(Fca)], 6.79 [d, $^3J_{HH}$ = 7.26 Hz, 1 H, NH(Ala)], 5.51 [br.s, 1 H, NH(Aib)], 4.74 [m, 2 H, Cp-H, CH(Ala)], 4.62 (s, 1 H, Cp-H), 4.61 (s, 1 H, Cp-H), 4.50 (s, 1 H, Cp-H), 4.39 (s, 1 H, Cp-H), 4.36 (s, 1 H, Cp-H), 4.10 (s, 1 H, Cp-H), 4.04 (s, 1 H, Cp-H), 3.81 (s, 3 H, OCH_3), 3.38 [m, 1 H, CH_2(Aib)], 3.27 [m, 1 H, CH_2(Aib)], 2.60 [m, 1 H, CH(Aib)], 1.44 [s, 9 H, CH_3(Boc)], 1.53 [d, $^3J_{HH}$ = 7.20 Hz, 3 H, CH_3(Ala)], 1.20 [d, $^3J_{HH}$ = 6.96 Hz, 3 H, CH_3(Aib)] ppm. $^{13}C\{^1H\}$ NMR ($CDCl_3$, 150 MHz): δ = 174.30 [s, CO(ester)], 173.42 [s, CO(amide)], 169.70 [s, CO(Fca)], 155.86 [s, CO(Boc)], 94.79 (s, Cp-C_q), 78.90 [s, C(Boc)], 75.65 (s, Cp-C_q), 70.98 (s, Cp-C), 70.73 (s, Cp-C), 69.56 (s, Cp-C), 69.05 (s, Cp-C), 65.60 (s, Cp-C), 65.27 (s, Cp-C), 64.06 (s, Cp-C), 62.78 (s, Cp-C), 52.14 (s, OCH_3), 47.63 [s, CH(Ala)], 43.33 [s, CH_2(Aib)], 41.41 [s, CH(Aib)], 27.94 [s, CH_3(Boc)], 17.26 [s, CH_3(Ala)], 15.20 [s, CH_3(Aib)] ppm. CV (CH_2Cl_2): $E_{1/2}$ = 90 mV vs. Fc/Fc^+.

Supporting Information (see footnote on the first page of this article): DFT-calculated Cartesian coordinates of conformers of **2**, **3**, **4** and **6** and CD spectra of **2**, **3**, **4** and **6** as KBr disks.

Acknowledgments

We thank the Ministry for Science, Education and Sport of Croatia for support through grant number 058-1191344-3122.

[1] D. Seebach, F. D. Hook, A. Glättli, *Biopolymers* **2006**, *84*, 23–37.
[2] R. P. Cheng, S. H. Gellman, W. F. DeGrado, *Chem. Rev.* **2001**, *101*, 3219–3232.
[3] R. L. Baldwin, G. D. Rose, *Trends Biochem. Sci.* **1999**, *24*, 77–83.
[4] R. Aurora, G. D. Rose, *Protein Sci.* **1998**, *7*, 21–38.
[5] D. Seebach, R. I. Mathad, T. Kimmerling, Y. R. Mahajan, P. Bindschadler, M. Rueping, B. Jaun, C. Hilty, T. Etezady-Esfarjani, *Helv. Chim. Acta* **2005**, *88*, 1696–1982.
[6] M. Rueping, J. V. Schreiber, G. Lelais, B. Jaun, D. Seebach, *Helv. Chim. Acta* **2002**, *85*, 2577–2593.
[7] G. Lelais, D. Seebach, *Biopolymers* **2004**, *76*, 206–243.
[8] H.-A. Klok, *Angew. Chem.* **2002**, *114*, 1579–1583; *Angew. Chem. Int. Ed.* **2002**, *41*, 1509–1513.
[9] D. Kanamori, T. Okamura, H. Yamamoto, N. Ueyama, *Angew. Chem.* **2005**, ***117***, 991–994; *Angew. Chem. Int. Ed.* **2005**, *44*, 969–972.
[10] D. J. Hill, M. J. Mio, R. B. Prince, T. S. Hughes, J. S. Moore, *Chem. Rev.* **2001**, *101*, 3893–4011.
[11] I. Huc, *Eur. J. Org. Chem.* **2004**, 17–29.
[12] a) T. Moriuchi, T. Hirao, *Chem. Soc. Rev.* **2004**, *33*, 294–301; b) T. Moriuchi, A. Nomoto, K. Yoshida, T. Hirao, *J. Organomet. Chem.* **1999**, *589*, 50–58; c) S. I. Kirin, H.-B. Kraatz, N. Metzler-Nolte, *Chem. Soc. Rev.* **2006**, *35*, 348–354.
[13] D. R. van Staveren, N. Metzler-Nolte, *Chem. Rev.* **2004**, *104*, 5931–5985.
[14] G. Hölzemann, *Kontakte (Darmstadt)* **1991**, *1*, 3–13.
[15] G. Hölzemann, *Kontakte (Darmstadt)* **1991**, *2*, 56–64.
[16] D. Obrecht, M. Altorfer, J. A. Robinson, *Adv. Med. Chem.* **1999**, *4*, 1–68.
[17] K. S. Kee, S. D. S. Jois, *Curr. Pharm. Des.* **2003**, *9*, 1209–1224.
[18] S. Chowdhury, D. A. R. Sanders, G. Schatte, H.-B. Kraatz, *Angew. Chem.* **2006**, *118*, 765–768; *Angew. Chem. Int. Ed.* **2006**, *45*, 751–754.
[19] T. Moriuchi, T. Nagai, T. Hirao, *Org. Lett.* **2005**, *7*, 5265–5268.
[20] S. I. Kirin, D. Wissenbach, N. Metzler-Nolte, *New J. Chem.* **2005**, *29*, 1168–1173.
[21] S. Chowdhury, G. Schatte, H.-B. Kraatz, *Dalton Trans.* **2004**, 1726–1730.
[22] F. E. Appoh, T. C. Sutherland, H.-B. Kraatz, *J. Organomet. Chem.* **2004**, *689*, 4669–4677.
[23] T. Moriuchi, K. Yoshida, T. Hirao, *Org. Lett.* **2003**, *5*, 4285–4288.
[24] T. Moriuchi, A. Nomoto, K. Yoshida, T. Hirao, *Organometallics* **2001**, *20*, 1008–1013.
[25] T. Moriuchi, A. Nomoto, K. Yoshida, A. Ogawa, T. Hirao, *J. Am. Chem. Soc.* **2001**, *123*, 68–75.
[26] R. S. Herrick, R. M. Jarret, T. P. Curran, D. R. Dragoli, M. B. Flaherty, S. E. Lindyberg, R. A. Slate, L. C. Thornton, *Tetrahedron Lett.* **1996**, *37*, 5289–5292.
[27] A. Nomoto, T. Moriuchi, S. Yamazaki, A. Ogawa, T. Hirao, *Chem. Commun.* **1998**, 1963–1964.
[28] S. I. Kirin, U. Schatzschneider, S. D. Köster, D. Siebler, N. Metzler-Nolte, *Inorg. Chim. Acta* **2009**, *362*, 894–906.
[29] L. Barišić, V. Rapić, H. Pritzkow, G. Pavlović, I. Nemet, *J. Organomet. Chem.* **2003**, *682*, 131–142.
[30] L. Barišić, M. Dropučić, V. Rapić, H. Pritzkow, S. I. Kirin, N. Metzler-Nolte, *Chem. Commun.* **2004**, 2004–2005.
[31] L. Barišić, M. Čakić, K. A. Mahmoud, Y. Liu, H.-B. Kraatz, H. Pritzkow, S. I. Kirin, N. Metzler-Nolte, V. Rapić, *Chem. Eur. J.* **2006**, *12*, 4965–4980.
[32] V. Kovač, K. Radolović, I. Habuš, D. Siebler, K. Heinze, V. Rapić, *Eur. J. Inorg. Chem.* **2009**, 389–399.
[33] M. Čakić Semenčić, D. Siebler, K. Heinze, V. Rapić, *Organometallics* **2009**, *28*, 2028–2037.
[34] K. Heinze, M. Beckmann, *Eur. J. Inorg. Chem.* **2005**, 3450–3457.
[35] K. Heinze, U. Wild, M. Beckmann, *Eur. J. Inorg. Chem.* **2007**, 617–623.
[36] L. Barišić, V. Rapić, V. Kovač, *Croat. Chem. Acta* **2002**, *75*, 199–210.

[37] G. Nagula, V. J. Huber, C. Lum, B. A. Goodman, *Org. Lett.* **2000**, *2*, 3527–3529.
[38] M. J. Frisch, G. W. Trucks, H. B. Schlegel, G. E. Scuseria, M. A. Robb, J. R. Cheeseman, J. A. Montgomery Jr., T. Vreven, K. N. Kudin, J. C. Burant, J. M. Millam, S. S. Iyengar, J. Tomasi, V. Barone, B. Mennucci, M. Cossi, G. Scalmani, N. Rega, G. A. Petersson, H. Nakatsuji, M. Hada, M. Ehara, K. Toyota, R. Fukuda, J. Hasegawa, M. Ishida, T. Nakajima, Y. Honda, O. Kitao, H. Nakai, M. Klene, X. Li, J. E. Knox, H. P. Hratchian, J. B. Cross, C. Adamo, J. Jaramillo, R. Gomperts, R. E. Stratmann, O. Yazyev, A. J. Austin, R. Cammi, C. Pomelli, J. W. Ochterski, P. Y. Ayala, K. Morokuma, G. A. Voth, P. Salvador, J. J. Dannenberg, V. G. Zakrzewski, S. Dapprich, A. D. Daniels, M. C. Strain, O. Farkas, D. K. Malick, A. D. Rabuck, K. Raghavachari, J. B. Foresman, J. V. Ortiz, Q. Cui, A. G. Baboul, S. Clifford, J. Cioslowski, B. B. Stefanov, G. Liu, A. Liashenko, P. Piskorz, I. Komaromi, R. L. Martin, D. J. Fox, T. Keith, M. A. Al-Laham, C. Y. Peng, A. Nanayakkara, M. Challacombe, P. M. W. Gill, B. Johnson, W. Chen, M. W. Wong, C. Gonzalez, J. A. Pople, *Gaussian 03*, Revision B.03, Gaussian, Inc., Pittsburgh PA, **2003**.

Received: November 25, 2009
Published Online: January 27, 2010

